Melting and freezing in isothermal Ar_{13} clusters

Heidi L. Davis, Julius Jellinek,[a] and R. Stephen Berry
Department of Chemistry and the James Franck Institute, The University of Chicago, Chicago, Illinois 60637

(Received 20 November 1986; accepted 20 February 1987)

Microcanonical simulations have shown that Ar_{13} clusters have sharp but unequal melting and freezing energies. Between these energies, a hot solid-like form and a cooler, liquid-like form coexist in dynamic equilibrium. Monte Carlo and isothermal molecular dynamics simulations confirm that this coexistence behavior persists under canonical conditions as well. Many properties demonstrate the solid and liquid character of the two coexisting "phases." One previous result seemed to contradict this: Quirke and Sheng evaluated nearest neighbor angular distribution function $P(\theta)$; its nonzero value for $\theta = \pi/2$ at 33 K was interpreted as that of a hot solid in a "premelting expansion." Actually, that result is the average of a bimodal distribution, one mode for the solid and the other for the liquid. The average shifts smoothly with T, and each form's $P(\theta)$ changes slightly with temperature. The solid has tiny nonzero probability for $\pi/2$. The liquid has a minimum probability there, but far above zero. Mean-square displacements and power spectra calculated at 33 K from the Nosé constant temperature molecular dynamics method exhibit properties which are clearly distinguishable and identifiable with two distinct phases, as they are under isoergic conditions. Hence our results can be added to the evidence supporting the picture for finite systems of two phases coexisting over a finite temperature and energy range.

I. INTRODUCTION AND MODEL

Computer simulations of Kristensen *et al.*,[1] Briant and Burton,[2] Kaelberer and Etters,[3] and McGinty[4] have indicated that free, argon-like clusters can exist in both solid- and liquid-like forms, and that the transition between these forms is much more complicated than the gradual, expansive type of phenomenon that might previously have been expected for such small systems. Berry *et al.*[5,6] have developed a quantum statistical model to provide insight into the observed melting behavior of these systems and in so doing have made some specific predictions. According to their "two-phase" model, a small, Ar-like cluster will, under isothermal isobaric conditions, exhibit sharp but unequal freezing and melting temperatures, called T_f and T_m, respectively; T_f is the lower bound of the stability of the liquid form and T_m is the upper bound of the stability of the solid form. For a system large enough to undergo a first-order phase transition, these temperatures necessarily coincide, but for small clusters, they bound a finite "coexistence region." For each temperature in this region, two stable forms of the cluster—one nearly rigid and solid-like, the other nonrigid and liquid-like—exist in stable equilibrium, in a temperature dependent distribution.

Extensive isoergic molecular dynamics (MD) studies of Jellinek, Beck, and Berry[7] (JBB) and Amar and Berry[8] have revealed that this type of coexistence behavior occurs for Ar_{13} and several other small isoergic Ar_n systems.[9] In this paper we report *isothermal* results for the Ar_{13} cluster which parallel those obtained by Jellinek, Beck, and Berry and provide the first direct evidence in support of the canonical two-phase model for such systems. Doing so, we naturally explain an apparent discrepancy in the Monte Carlo literature—namely that some structural data obtained by Quirke and Sheng[10] seemed to imply that the melting behavior of Ar_{13} occurs not with the rapid onset of a liquid phase, as suggested from the studies of Etters and Kaelberer[3] (and MD studies[2]), but as the gradual transformation of a single stable form with temperature. We will explicitly show that the results of Quirke and Sheng (QS) and Etters and Kaelberer (EK) are consistent and are consequences of a two-phase coexistence phenomenon, but first we review the microcanonical results of Jellinek, Beck, and Berry[7] for this system.

In isoergic MD simulations at low total energies, the Ar_{13} cluster exhibits a single stable form having the structural and dynamical characteristics of a solid; at significantly higher energies, only a liquid appears. For a finite range of intermediate energies, two forms having different mean potential energies appear in stable equilibrium. For every total energy in this intermediate range, the cluster spends a long enough part of the simulation time in each mean potential region to establish a temperature and other relevant properties characteristic of that phase. Long-time averages of relative bond length fluctuations, mean-square displacements and velocity autocorrelation functions indicate that the two "temperature forms" are distinct; one is liquid-like, the other solid-like. Temperature distributions obtained in this coexistence region are bimodal for Ar_{13} and other, but not all, small Ar_n clusters.[9] For all species exhibiting bimodal distributions, the probability of finding a cluster in a low temperature (high potential energy) form increases monotonically

[a] Present address: Chemistry Division, Argonne National Laboratory, Argonne, Illinois 60439.

 0021-9606/87/116456-09$02.10

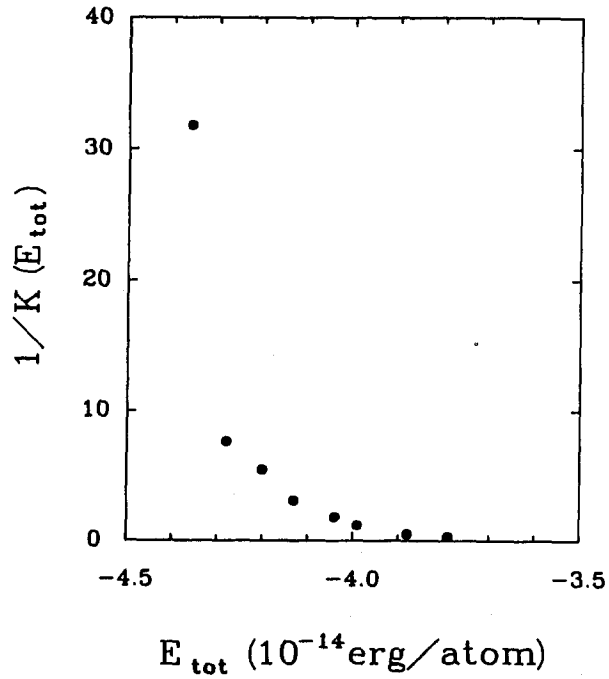

FIG. 1. The inverse equilibrium constant K_{eq}^{-1} = [solid]/[liquid] of Jellinek, Beck, and Berry given as a function of total energy. $K_{eq}(E_{tot})$ has been calculated by counting the number of time steps spent in each temperature form and taking the ratio of time spent in a liquid- to solid-like form. Values have converged to 3%. A discussion of this function's behavior near the end points is given in the text.

as a function ot total energy. (See Figs. 1 and 2.)

II. METHODS

We have employed both a Metropolis Monte Carlo algorithm[11] and the Nosé constant temperature MD method[12,13] for our simulations. The latter technique couples our physical system to a "bath" by adding an extra degree of freedom (more precisely, one pair of canonical variables) to Hamilton's equations in a manner which is guaranteed under the quasiergodic hypothesis to give canonical averages of static properties. It affords the additional opportunity of calculating some dynamical properties. These may be useful in distinguishing different potential energy forms as disparate phases and not simply different solid isomers.

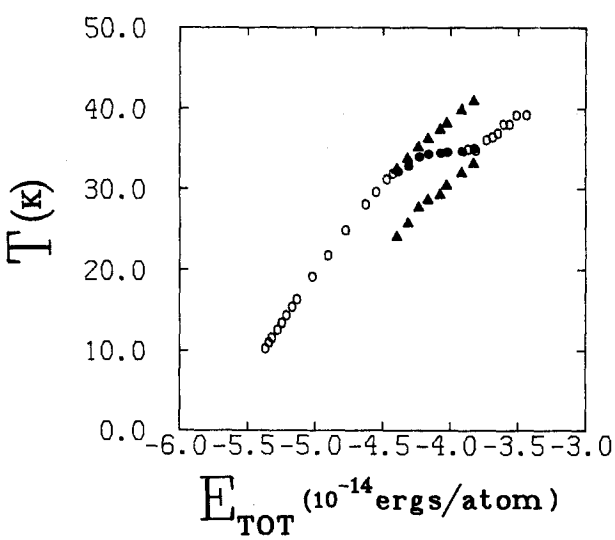

FIG. 2. Calorid curve produced from the isoergic study of Jellinek, Beck, and Berry. We have converted their kinetic energy values to those of temperature with the approximation $T = 2E_K/[(3N-6)k]$ so that their results may more easily be compared to ours. Circles represent data obtained over an entire MD simulation. For energies outside the coexistence region, open circles are used. Triangles represent temperatures calculated separately over each phase inside the "two-phase" region.

The Monte Carlo calculations were performed under the guidelines of Etters and Kaelberer.[14] A Lennard-Jones potential was used with the same parameters ($\sigma = 3.4\times10^{-8}$ cm, $\epsilon = 1.67\times10^{-14}$ erg) chosen by EK, QS, and JBB to simulate the interatomic potential of Ar. All runs consisted of at least 10^6 configurations; as many as 10^7 were used in some cases. For $T < 26$ K and $T > 37$ K, simulations were extended until final averages of the potential energy approached convergence to within 1%. For each intermediate temperature, a coexistence of two phases of the cluster was observed, and the potential energy, when averaged separately over each phase, also approached convergence to within 1%. Obtaining such a level of convergence for the potential energy fully averaged over both phases proved much more difficult than over single phases because it required not only that the potential energy calculated for each phase reach its equilibrium value to the desired degree of accuracy but also that the *distribution* of coexisting phases approach equilibrium as well. For most of our calculations, the expectation value of the fully averaged potential energy has only been obtained to within 2%.

Before presenting our results, it is worth mentioning a problem inherent to all Lennard-Jones, free boundary MC calculations; namely, the average potential energy of the entire system

$$\langle U\rangle = \sum_{i<j} \frac{\int_{-\infty}^{+\infty} U_{ij}(\mathbf{r}) e^{-U_{ij}(\mathbf{r})/kT}\, d\mathbf{r}}{\int_{-\infty}^{+\infty} e^{-U_{ij}(\mathbf{r})/k}T\, d\mathbf{r}} \tag{1}$$

vanishes in the limit of an infinite number of configurations. This problem corresponds physically to evaporation of atoms from the surface and is not unexpected. However, for most of our calculations—all started in configurations of the bound cluster—expectation values of physical properties could be obtained to within the desired degree of accuracy while the cluster remained in its "metastable" bound state.[15] At $T \geqslant 37$ K, combining the results of several "short" runs became necessary to obtain reasonable averages prior to evaporation.[16]

III. CALCULATIONS AND RESULTS

A caloric curve (Fig. 3) has been generated for the Ar_{13} system by plotting the total energy per atom, as obtained from each of our MC simulations, against temperature. For a range of temperatures $26 \leqslant T \leqslant 37$ K, the potential energy and the total energy are two-valued functions of temperature. We demonstrate in a later section that this range of temperatures comprises a coexistence region, like that predicted from the two-phase model of Berry *et al.* and observed during recent MD simulations of this system.[7,8]

The configurational heat capacity C is calculated as

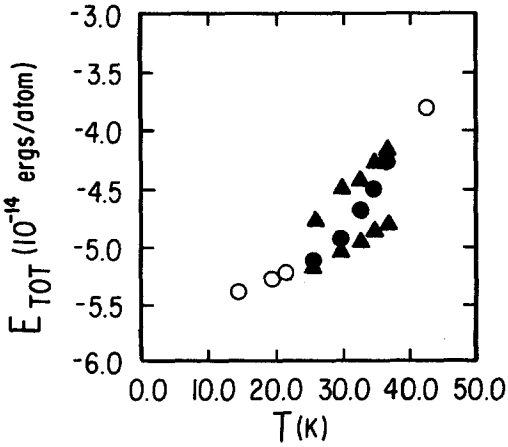

FIG. 3. To the potential energy derived from each MC simulation, we have added a kinetic energy (calculated from a direct scaling of temperature) to produce a caloric curve of total energy as a function of temperature. The coexistence end points have not yet been determined precisely. See caption under Fig. 2 for key.

$$C = \frac{\langle U^2 \rangle - \langle U \rangle^2}{kT^2}, \tag{2}$$

where $\langle\ \rangle$ represents the averaging over an entire MC simulation. C is given as a function of temperature in Fig. 4. For temperatures near 20 K, the value of the configurational heat capacity is approximately 3×10^{-15} ergs/K. Near 26 K, this function begins to increase steeply, reaching roughly five times its former value at a temperature of 35 K. Our curve of $C(T)$ is much like that obtained for this system by Quirke and Sheng.[10] Its smooth, broad shape led Quirke and Sheng to argue that no familiar, abrupt phase transition was occurring for this system. However its broad peak is consistent with the finite coexistence range observed for this system and predicted from the model of Berry *et al.*[5,6]

For a system as small as 13 particles, the correlation between results obtained from microcanonical and canonical ensembles is not necessarily trivial. However, our caloric curve is very closely the inverse of that obtained from the isoergic studies of JBB. Figure 5 compares our results.

Extending the two-phase model and its notation to the

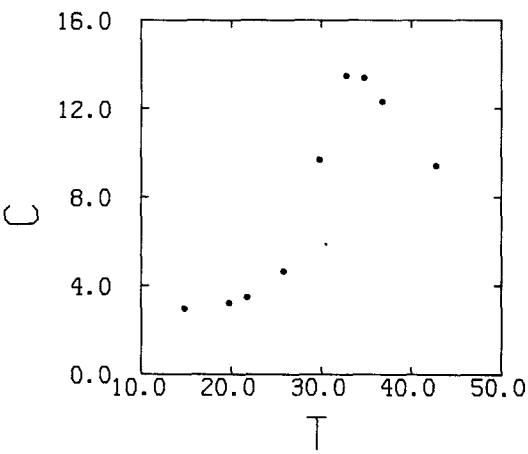

FIG. 4. Configurational heat capacity given as a function of temperature, expressed in units of 10^{-15} ergs/K.

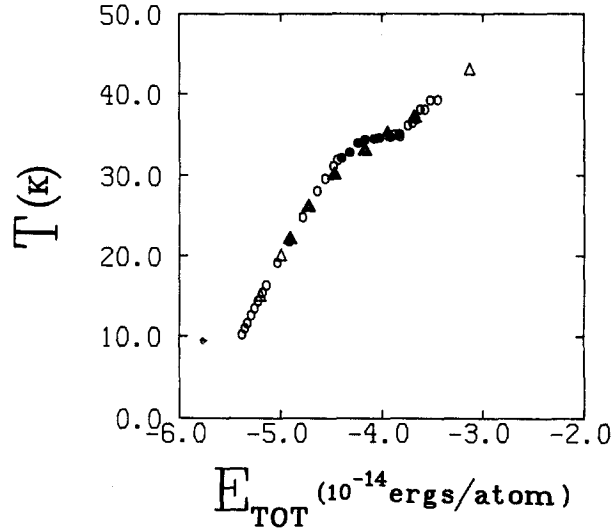

FIG. 5. Our total energy values (△) superimposed onto the caloric curve of Jellinek, Beck, and Berry (○). All points represent averages over entire simulations; for darkened points this implies a combined average over coexisting forms.

microcanonical ensemble, one would expect the caloric curve of JBB to jump or at least change slope abruptly at the freezing E_f and melting E_m total energies, reflecting discontinuities in the equilibrium constant $K_{eq}(E)$ at these points.[6,7] Given the numerical limitations on the resolving power of these calculations and the fact that the predicted discontinuity in the equilibrium constant could be extremely small, the shape of the caloric curve is not unreasonable; the general differences between the coexistence and single-phase regions in their curve are evident.

It is straightforward to observe coexistence using either constant energy or isothermal MD calculations. For constant temperature calculations, short-time averages of the potential energy can be obtained over a few of the cluster's breathing periods; when plotted against time, these separate into distinct bands, each of which is easily distinguished by eye and usually shows the cluster staying in a particular potential energy region for times long, relative to its characteristic breathing period. (See Fig. 6.)

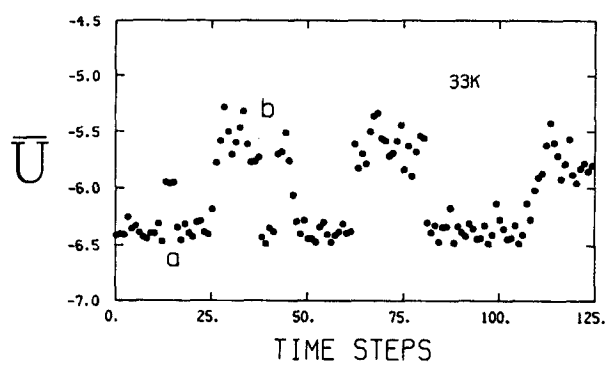

FIG. 6. Short-time potential energy averages vs time for a typical Nosé type simulation of coexistence behavior. Each point represents an average over 1800 steps, each of which is 0.003 ps so that each point represents roughly three of the cluster's characteristic breathing periods. Energy is in units of 10^{-14} ergs. Here, $Q = 200$ Å amu^2. Points in region (a) represent the solid-like form of the cluster; those in region (b) are $\bar{U}$ obtained over the liquid-like "phase."

A more systematic means of separation is obtained by calculating a distribution for these short-time averages of potential energy ($\overline{U}$). For temperatures in the coexistence region, such a $\overline{U}$ distribution appears bimodal. In fact, the bimodality of the distribution provides a practical criterion for distinguishing coexistence, as Fig. 7 shows. The minimum of this distribution is chosen as the separation value of $\overline{U}$, or separatrix.[17] When the calculation is repeated a mean potential energy and various other physical properties are averaged over each short-time interval. The value of $\overline{U}$ for each interval is compared to the separatrix. If less, averages of the properties calculated over this interval are stored in the low potential energy "bin;" otherwise, calculated properties are stored in the high potential energy bin. At the end of the simulation, the short-time averages for each property are averaged over each bin separately, allowing both parts of the distribution to be characterized individually.

The MC calculations do not provide the dynamics which yield such a convenient separation of time scales (especially with the magic number clusters) in the MD simulations. In the MC scheme, the short-time potential energy averages are really averages over a few thousand configurations, unrelated by any dynamics, and although some diffuse bands do emerge when these are plotted sequentially, the coexisting forms are difficult to distinguish unambiguously until one invokes a more precisely defined separation scheme like the abovementioned. For our calculations, the short intervals typically consist of 3500 configurations. However, for the coexistence temperatures studied, changing this interval to 2000 or 5000 configurations does change the mean potential energy associated with each mode of the distribution or the relative areas of the two peaks. When the value of the short interval is chosen much less than 3500, the calculated $\overline{U}$ are widely dispersed, and it becomes difficult or impossible to observe any banding in plots of sequential values of $\overline{U}$. If too large an interval is chosen, the calculated $\overline{U}$ are likely to contain contributions from each of the coexisting forms of the cluster, resulting in an inefficient separation of data. It is then not surprising that previous researchers have overlooked the coexistence or two-phase phenomenon.

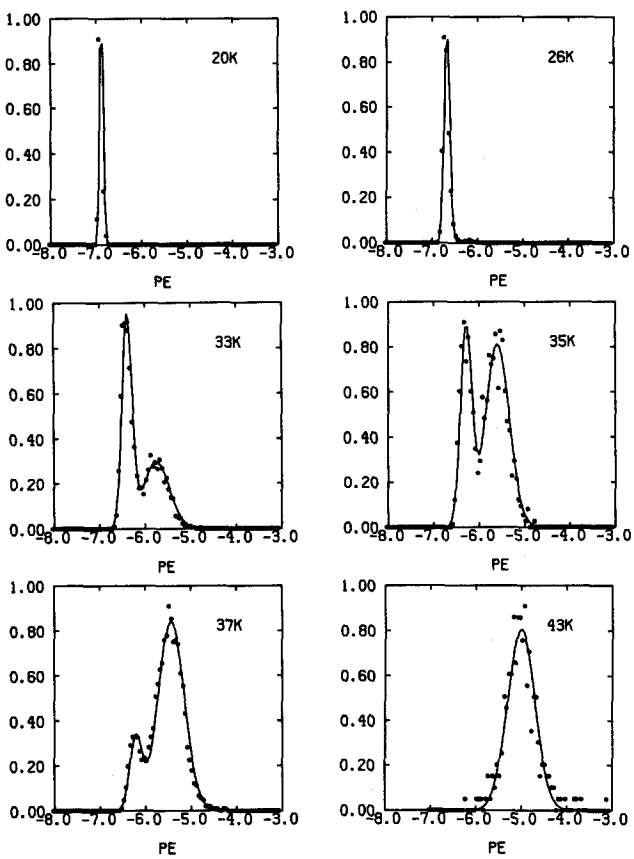

FIG. 7. Distributions of $\overline{U}$ values which have been averaged over a small number of configurations (typically 3500) using MC sampling. The solid line represents a "best fit" curve to the sum of two Gaussians, except for temperatures of 20 and 43 K, where the curve represents a fit to a single Gaussian. For each temperature, the center(s) of the "fit" Gaussian(s) compares well to the final potential energy average(s) calculated directly from the program (as the arithmetic mean over a given phase); see Table I.

Without the idea of coexisting phases, the competing data of EK and QS are difficult to reconcile. The results of EK are presented in terms of a single melting temperature, occurring for this system near 29 K. If, indeed, there is a transition from pure solid to pure liquid at this temperature, QS emphasize that structural data, in particular the angular distribution function, obtained at higher temperatures should be indicative of a liquid.[10]

The angular distribution function (adf) gives the average probability of finding nearest neighbors at a given angle about the center particle; this distribution provides a particularly good structural probe of the 13-particle cluster. In its most rigid, icosahedral form, the cluster produces sharp maxima in the adf for 60° and 120° nearest neighbor angles but is even better characterized by an absence of probability for the angle of 90°. A hot, liquid cluster exhibits a more uniform angular distribution, although peaks at 60° and 120° still appear.

We obtained results for 33 K, shown in Fig. 8, that are essentially identical to those of Quirke and Sheng.[10] Not realizing this temperature falls within a "coexistence" region, QS inferred from the adf that this distribution is one of a "hot" solid, occurring with the (smooth) onset of a "premelting expansion." Certainly, it is not representative of a pure liquid.

What the fully averaged adf shows at this temperature is the combination of contributions from the two potential energy forms. When the data for these forms are separated, very different angular distribution functions emerge. The high-potential energy form produces less dramatic peaks in the adf at 60° and 120° and a significantly higher probability at 90° than does the more rigid low-potential energy form. Similar results are obtained for each temperature in the coexistence range. The 90° probability for the combined angular distribution function $P_c(90)$ increases, as one expects, as the temperature dependent equilibrium constant $K_{eq}(T)$ increases. Looking at the separated distributions at each temperature, we find some mode softening occurring with the melting phenomenon which also contributes to $P_c(90)$. Because the two Gaussians approximating our $\overline{U}$ distributions in the coexistence range are typically overlapping, some of this softening is a numerical artifact of our imperfect separa-

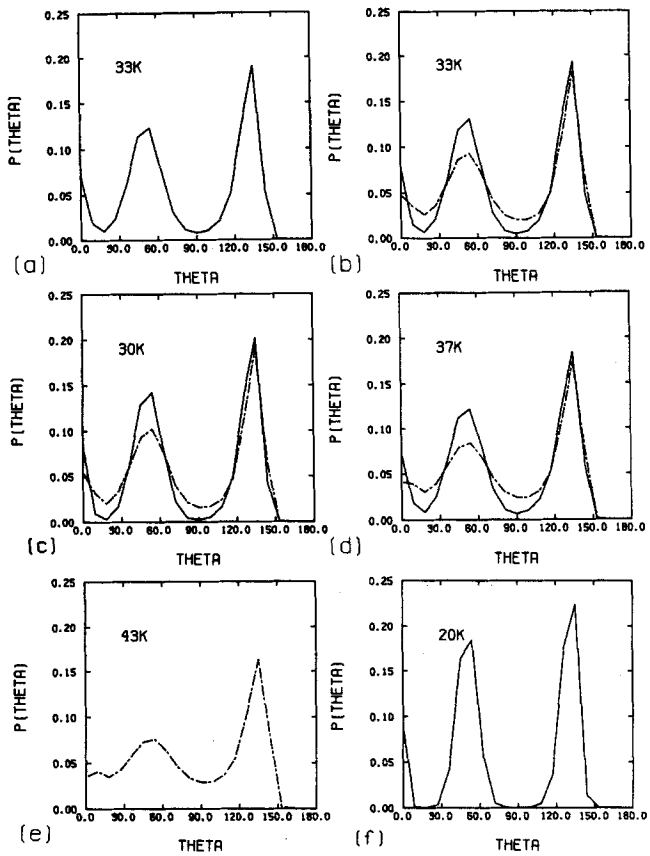

FIG. 8. (a) The angular distribution function (adf) calculated over all configurations during a 33 K MC simulation. (b) The adf data obtained separately over each of the low- and high-potential energy forms; the dashed curve represents the distribution of the higher potential energy (liquid) form. (c); (d) adf functions obtained over separate phases for coexistence temperatures of 30 and 37 K, respectively. (e); (f) Angular distribution functions of a pure liquid (dashed curve) at 43 K and a pure solid at 20 K.

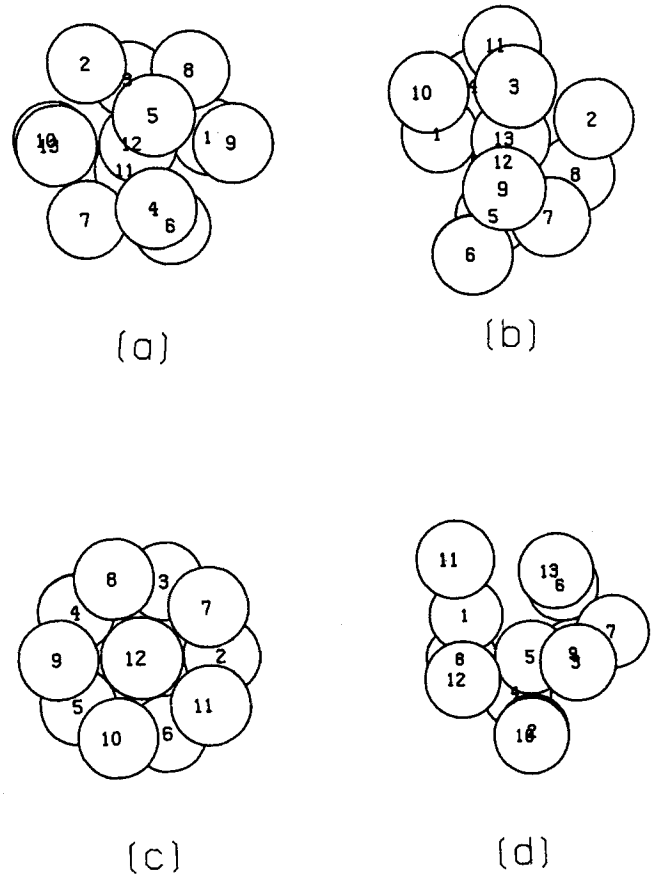

FIG. 9. "Snapshots" obtained from Nosé type MD simulations of the 13-particle Ar cluster. (a) and (b) are clusters obtained from the regions analogous to those labeled in Fig. 6, at 33 K. Compared to (c), which has been obtained from a 20 K simulation and is near the potential energy minimum, (a) has lost some of its icosahedral symmetry. (b) bears little resemblance to the clusters obtained at temperatures below T_f. The cluster labeled (d) is typical of that observed at 43 K; no underlying icosahedral symmetry is present. Similar observations are made from the MC data.

tion scheme, but there are other indications that much of this effect is real.

We have taken "snapshots" of our cluster by extracting and plotting the coordinates at random points during both the MC and MD simulations. Snapshots taken at temperatures of 15, 20, and 22 K reveal a very rigid, solid cluster with near icosahedral symmetry, like that shown in Fig. 9(a). At very high temperatures, an amorphous cluster is obtained whose particles frequently interchange. Within the coexistence range, an analog to the solid cluster is observed in the low potential energy regions; it displays some symmetry, but is no longer a regular icosahedron and is more expanded than the pure solid form. The high-potential energy forms are much less rigid; however, they do not undergo particle interchange as often or appear as structureless as the clusters do at pure-liquid temperatures.

Looking at the relative bond length fluctuation as a function of temperature points up the sharpness of the coexistence boundaries for this system. The rms bond length fluctuation δ, which indicates the mobility of atoms in the cluster, is calculated as

$$\delta = \frac{2}{N(N-1)} \sum_{i<j} \left(\frac{\langle \mathbf{r}_{ij}^2 \rangle - \langle \mathbf{r}_{ij} \rangle^2}{\langle \mathbf{r}_{ij} \rangle^2} \right)^{1/2}, \qquad (3)$$

where $\langle\ \rangle$ denotes, respectively, an ensemble or time average over either an entire MC or MD simulation. Our results, given in Fig. 10 as a function of temperature, are similar to those obtained by EK[3] and JBB.[7] Although our curve is somewhat incomplete, it clearly displays a dramatic change in the dynamics of the cluster occurring over a narrow range of temperatures. The sharp increase in δ occurs remarkably close to the 0.1 value corresponding to the Lindemann criterion for melting.[18]

Our $\delta(T)$ curve appears shifted to lower temperatures relative to those of EK and JBB. The discrepancy between our results and those of Etters and Kaelberer is most likely due to their running much shorter simulations below 29 K.[3] $K_{eq}(T)$ is sufficiently small near T_f to require simulations of very many configurations (10^7 and greater) for the liquid-like phase to be adequately reflected in the $\delta(T)$ data. (See Table I.)

That the $\delta(T)$ curve of Jellinek, Beck, and Berry differs from ours is a direct consequence of the two studies sampling different ensembles. In the microcanonical study, $\delta(T)$ is plotted against a temperature $T(E)$ which has been averaged over an entire simulation. The lowest temperature at

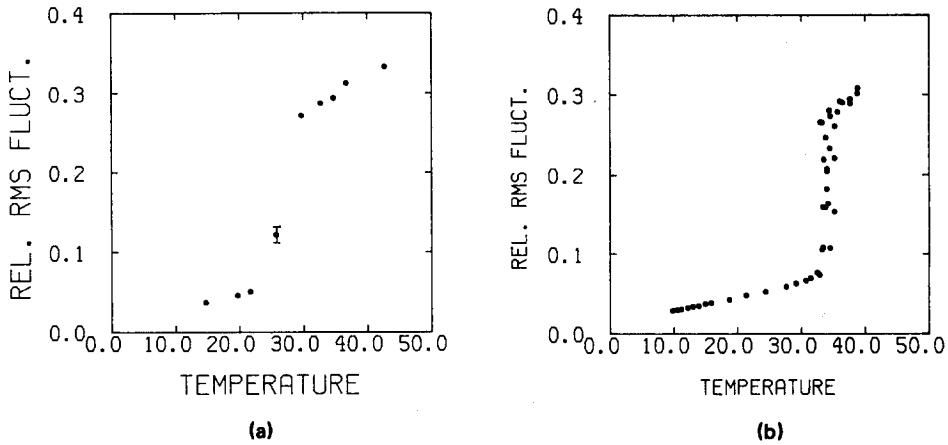

FIG. 10. (a) rms bond length fluctuations calculated from our MC studies and (b) those obtained from the microcanonical simulations of Jellinek, Beck, and Berry. Temperature is given in degrees Kelvin.

which JBB observe the largest increase in the curvature of $\delta(T)$ is roughly 33 K. This agrees well with the fully averaged temperature $T(E_f)$ corresponding to their reported freezing energy. However, it is $T_{\rm liq}(E_f)$, the average temperature of the nonrigid (higher potential energy) form at this energy, which should be compared with the temperature at which the curvature increases most rapidly (presumably, T_f) in the canonical study. This difference in temperatures $[T(E_f) - T_{\rm liq}(E_f)]$ is approximately 7 K and comparable in magnitude to the observed shift in our $\delta(T)$ results.

Figure 11 shows the equilibrium constant as a function of temperature inside the coexistence region. As mentioned earlier, very long simulations are required to calculate $K_{\rm eq}(T)$ to a high degree of accuracy. The "final" values of $K_{\rm eq}$ given in Fig. 11 agree within 5%. A rough estimate of $K_{\rm eq}$ can be calculated for each coexistence temperature from the relative areas of each Gaussian in the bimodal $\overline{U}$ distribution. The agreement between the values of $K_{\rm eq}(T)$ averaged directly from the simulations and the approximate values obtained from the MC $\overline{U}$ distributions is quite good, as Table I indicates.

IV. NOSÉ'S METHOD AND RESULTS

A description of our isothermal MD calculations is given in the Appendix. The remarkable feature of Nosé's method is that it is capable (in principle) of producing canonical ensemble averages of physical quantities from time averages calculated along continuous, deterministic trajectories. More precisely, one can obtain these averages for equilibrium quantities, as shown by the comparison in Table II between our MC and constant temperature MD calculations of mean potential energy.

The applicability of Nosé's method for the calculation of time-dependent functions is not as straightforward. On a very short time scale, the dynamics induced by this method are directly related to an arbitrary "pumping" variable Q which controls the rate of heat exchange between the physical system and bath. However, some dynamic quantities seem fairly insensitive to Q. Nosé has found this to be the case for a system of (108) Ar-like particles at $V = 29.88$ cm^3 mol^{-1} and a bath temperature (T_b) of 150 K.[12] For fairly short runs, variation of Q induced differences in the "noise" associated with the mean-square displacement function but yielded the basically the same underlying curve of displacements. Diffusion coefficients calculated for Q's ranging from 1 to 100 agreed to within 20%.

Nosé has pointed out that velocity autocorrelation functions obtained from this method with different values of Q are identical to those calculated from isoergic MD methods to within statistical errors.[13] Evans and Holian have since shown that the effect of the constant temperature bath on the physical system produces deviations from the microcanoni-

TABLE I. Equilibrium constants $K_{\rm eq}$ = (liquid)/(solid) obtained directly from MC simulations compared to those calculated from the $\overline{U}$ distribution results.

	$K_{\rm eq}$	
T (K)	Simulation	Distribution
30	1.8×10^{-1}	1.7×10^{-1}
33	5.7×10^{-1}	4.9×10^{-1}
35	1.9	1.5
37	5.7	5.3

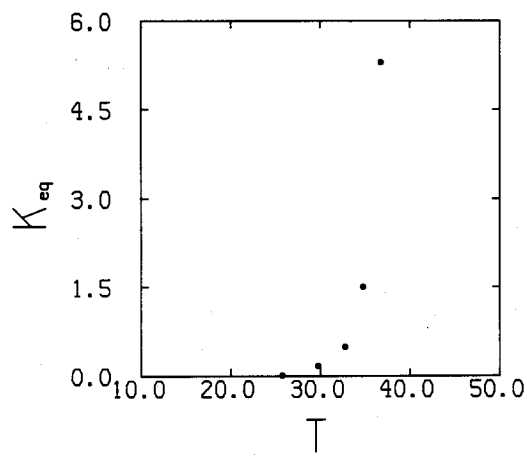

FIG. 11. $K_{\rm eq}(T)$ = [liquid]/[solid] from our MC simulations. T is in units of Kelvin. $K_{\rm eq}(26)$ has been obtained only to within 10%. Otherwise, data is reliable to within 5%.

TABLE II. Comparison of potential energy averages obtained directly from MC and MD[a] programs and those derived from the maxima of $\overline{U}$ distributions.[b]

	Potential energy (10^{-12} ergs)					
	Solid			Liquid		
T (K)	$\overline{U}$ distr.	MC	MD	$\overline{U}$ distr.	MC	MD
15	−0.701	−0.702	−0.702			
20	−0.687	−0.687	−0.687			
30	−0.651	−0.649		−0.606	−0.585	
33	−0.644	−0.634	−0.635	−0.574	−0.568	−0.569
35	−0.628	−0.625		−0.560	−0.567	
37	−0.621	−0.620		−0.544	−0.542	
43				−0.500	−0.497	

[a] MD data represent averages over the results from trajectories with $Q = 2$, $Q = 50$, and $Q = 200$ amu Å^2, although average potential energies obtained at all values of Q were very similar. See Table III.

[b] $\overline{U}$ distributions were generated from MC calculations, as described in the text.

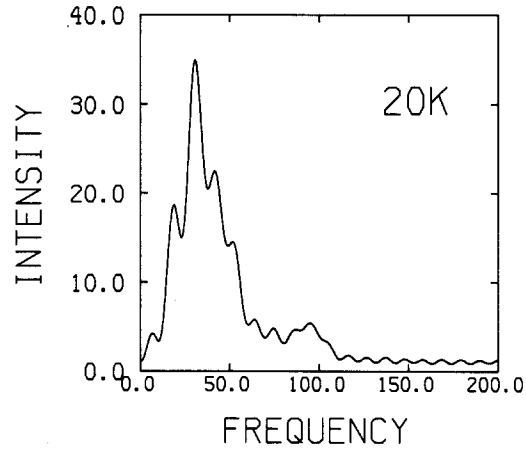

FIG. 12. Power spectrum obtained using the Nosé MD method with $T_b = 20$ K. Data shown have been obtained for $Q = 100$ amu Å^2. Frequency is in units of 10^{11}/s; intensity has units of 10^{-14}s.

cal correlation functions of the order $O(1/N)$,[20] so that the response functions for the linear region are well represented in the large-N (i.e., "thermodynamic") limit. However, this theorem is not strong enough to justify assuming, prior to the calculations, that our results for Ar_{13} or other small clusters would be within fluctuations of those predicted from isoergic MD calculations of Jellinek, Beck, and Berry, nor was it obvious that, for our purposes, our results would be sufficiently insensitive to Q. As we shall see below, the correlation functions from isoergic and isothermal MD simulations are entirely consistent, suggesting that the Evans-Holian result for infinite systems is also a useful approximation even for N as small as 13.

Because dynamical results were to be validated by comparison with several values of Q at each temperature, the method became costly. Therefore, we performed Nosé simulations only at 20 and 33 K; the latter provided a typical coexistence simulation and was adequate to show that the coexisting forms exhibit dynamics and structural properties which are substantially different.

As seen in Table II, potential energy averages obtained from this method and from the MC calculations are in good agreement. Table III shows that the calculated potential energy values are fairly insensitive to changes in the parameter Q.

For $T_b = 20$ K, the power spectra (calculated as the Fourier transforms of the respective velocity autocorrelation functions) obtained for simulations with $Q = 1$ and $Q = 100$ amu Å^2 are in close agreement with each other and with the typically solid spectrum obtained for this system under microcanonical conditions. As seen in Fig. 12, there is only a slight intensity at zero frequency, and a well-defined peak at $\omega = 40 \times 10^{11}$/s. The diffusion constant (D) for this system is likewise typical of a solid system. The values of D calculated using $Q = 1$ and $Q = 100$ amu Å^2 are 6.0×10^{-6} and 6.2×10^{-6} cm^2/s, respectively.

A coexistence of two potential energy forms of the cluster could be observed at 33 K. Figure 6 shows the short-time potential energy averages as a function of time for $Q = 200$ amu Å^2. As Q is changed the rate of "jumping" between potential energy forms changes, but again, the average values of potential energy do not. Because the value of the fully averaged potential energy is rigorously independent of Q, the ratio of time spent in the different potential energy forms must also be independent of this parameter. As Table IV illustrates, the agreement between K_{eq} values obtained at different Q's is somewhat poor, as is the agreement between these values and the MC result for $K_{eq}(33)$. The Nosé simulations have not been carried long enough in this case for the distribution of the two coexisting forms to reach its equilibrium value.

Calculations at $T_b = 33$ K have been performed for $Q = 2$, 50, 200, and 1000 amu Å^2. If a value much less than 2 amu Å^2 is entered into the MD program, the system be-

TABLE III. Average potential energy values obtained over respective phases during Nosé MD calculations with $T_b = 33$ K and various values of Q.

Q amu Å^2	Potential energy (10^{-12} ergs)		
	Solid	Liquid	Total
2	−0.635	−0.569	−0.617
50	−0.636	−0.570	−0.614
200	−0.635	−0.569	−0.616
1000	−0.637	−0.573	−0.621

TABLE IV. K_{eq} obtained from the Nosé MD method with $T_b = 33$ K and various values of Q. The respective K_{eq} from MC calculations is 5.7×10^{-1}.

Q (amu Å^2)	K_{eq}
2	3.6×10^{-1}
50	4.4×10^{-1}
200	4.0×10^{-1}
1000	3.4×10^{-1}

comes unstable, and the integration step size must be reduced to maintain a constant level of accuracy; for Q on the order of 1000 amu Å^2 or larger, coupling between the "heat reservoir" and the system is inefficient, and the coexisting forms exhibit significantly different temperatures. (See Table III.) The power spectra are virtually identical for all the tested values of Q. Those calculated for the low potential energy, rigid form of the cluster display few low frequency modes. The spectra of the high-potential form show more diffusive motion, as expected for a liquid. (See Figs. 13 and 14.)

At 33 K, the mean-square displacement functions, shown in Fig. 15, appear sensitive to the parameter Q. It is plausible that the differences in these curves arise because the efficiency of the calculational scheme used to separate the data for the two coexisting forms is itself a function of Q. Nonetheless, for each Q considered, D calculated for the lower potential energy form D^{low} is significantly greater than D^{high}. (See Table V.)

For each value of Q, the temperature associated with the system quickly equilibrates to that of the bath. Such a thorough equilibration is not always achieved (separately) for each coexisting form of the cluster at 33 K, as seen in Table III. Nosé has shown that the frequency (ω) of heat exchange between the physical system and the bath is proportional to $T/\sqrt{Q}$. Thus, for a given temperature, ω increases with decreasing Q. That the high potential energy form attains an average temperature greater than 33 K for $Q = 1000$ amu Å^2 is an indication that it is exchanging energy with the bath better than is the low potential energy form. Similarly, the low potential energy form exchanges heat with the reservoir more readily for lower values of Q. This observation is consistent with the high potential energy form undergoing softer, lower frequency vibrations than the low potential energy form and provides further suggestion that what we are observing at this temperature is the coexistence of two distinct phases of the 13-particle Ar cluster.

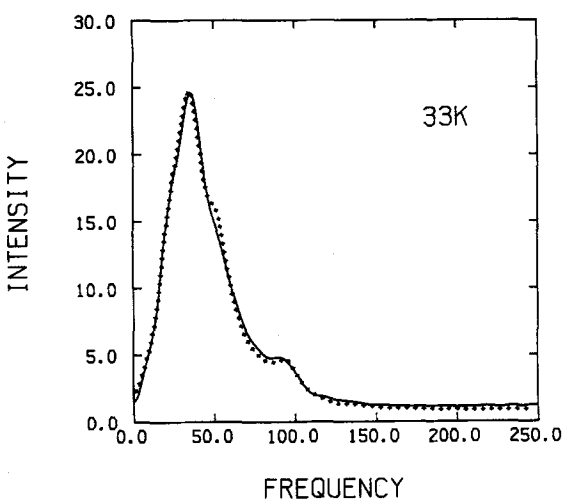

FIG. 13. Power spectra form the Nosé MD calculations with $T_b = 33$ K; $Q = 2$ (solid curve) and 200 (+) amu Å^2. Frequency is in units of 10^{11} s.$^{-1}$ Data represents the low-potential energy form of the cluster exclusively.

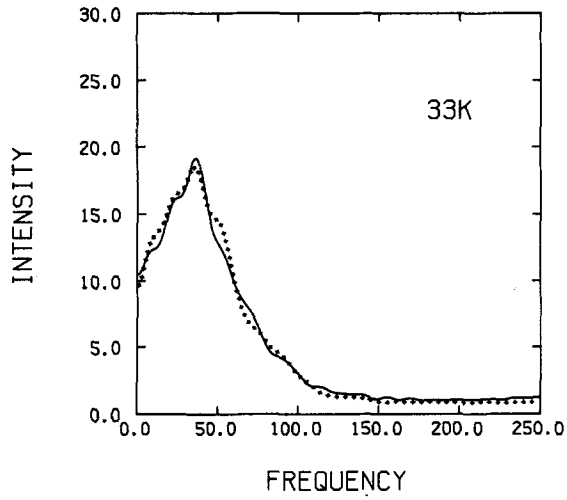

FIG. 14. Power spectrum calculated for the high-potential energy form of the cluster at 33 K. See Fig. 13 for key.

V. CONCLUSION

The objective of this paper has been to test whether the coexistence behavior observed in microcanonical studies for several small Ar_n systems does occur under canonical conditions, at least for the 13-particle system. Doing so, we have provided a necessary assay of the two-phase melting and freezing model proposed by Berry *et al.* However, several important questions remain. It is of particular interest to obtain a better estimate of how sharp the coexistence endpoints really are. Although many very long simulations would be necessary to calculate accurately the temperature boundaries of the coexistence region, knowing this temperature width to within a degree or less is very important for both a comparison between the microcanonical and canonical results for this system and for the understanding of the

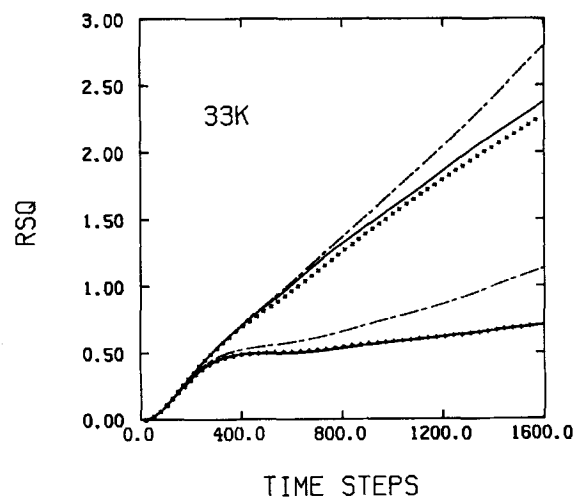

FIG. 15. Mean-square displacement (RSQ) as a function of time calculated for each of the coexisting forms of the cluster at $T_b = 33$ K and various values of Q. The RSQ function indicates the mobility of the cluster. Its long-time slope, which is consistently larger for the liquid-like cluster than for the solid, is directly proportional to the diffusion constant. Data for $Q = 50$ amu Å^2 are indicated by the dashed curve. Otherwise, notation is as in Fig. 13. Units for RSQ are Å^2; length of time step is 0.003 ps.

TABLE V. Diffusion constants and temperatures averaged over each phase for several values of Q, with $T_b = 33$ K.

Q amu Å^2	T (K)		D (10^{-5} cm^2/s)	
	Solid	Liquid	Solid	Liquid
2	33.00	33.00	4.4	6.9×10^{-1}
50	33.02	32.99	6.5	2.0
200	33.13	32.95	4.1	7.2×10^{-1}
1000	32.76	33.69	5.9	2.4

size dependence of the two-phase melting phenomenon.

Although one expects the temperature width (ΔT_c) of the coexistence region to decrease as the number of particles in the cluster increases,[6,7] the variation of $\Delta T_c(N)$ need not be monotonic with N. Recent isoergic studies by Beck, Jellinek, and Berry suggest that the behavior of corresponding energy width $\Delta E_c(N)$ is quite complicated.[9,19] ΔE_c for the 13-particle cluster is large compared to ΔE_c for other small clusters. The exceptional width of the coexistence region for the 13-particle system can be rationalized by the special stability of the icosahedral ground state with respect to structural rearrangements. The shapes of the potential surfaces of Ar_{13} and some other small clusters allow for a clean separation of time scales between the interval required for establishing the properties of the cluster within the region associated with one phase and the mean time to pass from one phase to the other, either during a coexistence simulation or, presumably, the real world.

For other clusters, where this separation of time scales is not so clear, we must better understand the dynamics of the systems before we can draw conclusions about their melting and freezing properties. For this reason, isoergic MD simulations, based on well-understood Hamiltonians, seem to be the tool of choice for further research on phenomena involving rate processes.

ACKNOWLEDGMENTS

This research was supported by a Grant from the National Science Foundation. Also, the authors wish to thank T. L. Beck, B. L. Holian, and N. Quirke for helpful discussions.

APPENDIX

The Nosé constant temperature MD method has been extensively reviewed.[20–23] We note here that we have employed the "real variable" version of this method. The equations of motion in this formalism are:

$$H_{\text{ext}} = \sum_{i=1}^{N} \frac{p_i^2}{2m_i} + \Phi(\{\mathbf{q}_i\}) + \frac{p_s^2 s^2}{2Q} + fkT_b \ln(s), \tag{A1}$$

$$\frac{d\mathbf{q}_i}{dt} = \frac{\mathbf{p}_i}{m_i}, \tag{A2}$$

$$\frac{d\mathbf{p}_i}{dt} = -\frac{\partial\Phi}{\partial\mathbf{q}_i} - \frac{sp_s\mathbf{p}_i}{Q}, \tag{A3}$$

$$\frac{ds}{dt} = \frac{p_s s^2}{Q}, \tag{A4}$$

$$\frac{dp_s}{dt} = s^{-1}\sum_{i=1}^{N}\left(\frac{\mathbf{p}_i^2}{m_i} - fkT_b\right) - \frac{sp_s^2}{Q}, \tag{A5}$$

where the scalar, dimensionless variable s and its conjugate momentum p_s represent a thermal bath. Q can be thought of as a mass for the degree of freedom s and is in fact a free parameter; $f = 3N - 6$ in our case, where N is the number of particles in the physical system. T_b is an external parameter which is interpreted as the temperature of the bath.

With a Hamming's fourth-order predictor–corrector program, time steps as small as 0.003 ps were typically required to conserve H_{ext}, the linear momentum and the angular momentum (in the center of mass of the physical system) to within five significant decimal places.

[1]W. D. Kristensen, E. J. Jensen, and R. M. J. Cotterill, J. Chem. Phys. **60**, 4161 (1974).
[2]C. L. Briant and J. J. Burton, J. Chem. Phys. **63**, 2045 (1975).
[3]J. B. Kaelberer and R. D. Etters, J. Chem. Phys. **66**, 3233 (1977); R. D. Etters and J. B. Kaelberer, *ibid.* **66**, 5112 (1977). (In this second paper, Etters and Kaelberer note the data suggest a coexistence of two phases, but the point is not pursued.)
[4]D. J. McGinty, J. Chem. Phys. **58**, 4733 (1973). Although McGinty reported only a gradual transition between the two limiting forms, he did observe a cluster with solid-like motions at low temperatures and, at higher temperatures, a cluster with liquid-like motions. See also Ref. 7.
[5]G. Natanson, F. Amar, and R. S. Berry, J. Chem. Phys. **78**, 399 (1983).
[6]R. S. Berry, J. Jellinek, and G. Natanson, Phys. Rev. A **30**, 919 (1984); Chem. Phys. Lett. **107**, 227 (1984).
[7]J. Jellinek, T. Beck, and R. S. Berry, J. Chem. Phys. **84**, 2783 (1986).
[8]F. Amar and R. S. Berry, J. Chem. Phys. **85**, 5774 (1986).
[9]T. L. Beck, J. Jellinek, and R. S. Berry, J. Chem. Phys. (in press).
[10]N. Quirke and P. Sheng, Chem. Phys. Lett. **110**, 63 (1984).
[11]Good descriptions of the Metropolis and general MC methods can be found by J. P. Valleau and S. G. Whittington, in *Modern Theoretical Chemistry, Part A*, edited by B. Berne (Plenum, New York, 1977), Vol. 5, Chaps. 4 and 5; and by W. W. Wood, in *Physics of Simple Liquids* (North-Holland, Amsterdam, 1968).
[12]S. Nosé, Mol. Phys. **52**, 255 (1984).
[13]S. Nosé, J. Chem. Phys. **81**, 511, (1984).
[14]R. D. Etters and J. Kaelberer, Phys. Rev. A **11**, 1068 (1975).
[15]For further discussion, see R. S. Berry, T. L. Beck, H. L. Davis, and J. Jellinek, in *The Evolution of Size Effects in Chemical Dynamics*, Advances in Chemical Physics, edited by I. Prigogine and S. A. Rice (Wiley, New York) (in press).
[16]This problem arises in the MD simulations as well. Jellinek, Beck, and Berry find calculations difficult at total energies above -3.61×10^{-14} ergs/atom, which corresponds to an average temperature of 37 K. See Ref. 7.
[17]This selection of the separation $\overline{U}$ is coarse, but is much cheaper computationally than more accurate, alternative methods.
[18]I. Z. Fisher, *Statistical Theory of Liquids* (University of Chicago, Chicago, 1966).
[19]T. Beck and R. S. Berry (in preparation).
[20]D. J. Evans and B. L. Holian, J. Chem. Phys. **83**, 4069 (1985).
[21]W. G. Hoover, Phys. Rev. A **31**, 1695 (1985).
[22]D. J. Evans and G. P. Morriss, Comput. Phys. Rep. **1**, 272 (1984).
[23]J. Jellinek and R. S. Berry (to be published).